



OPEN **GA BP prediction model for energy consumption of steel rolling reheating furnace**

Yi Duan, Guang Chen, Xiangjun Bao[✉], Jing Xu, Lu Zhang & Xiaojing Yang

Energy consumption serves as a critical indicator of energy utilization efficiency and environmental sustainability in the steel production process. Accurately predicting the Heat energy consumption per ton (HEC, GJ/t) of steel billet in Steel Rolling Reheating Furnace (SRRF) presents a formidable challenge owing to the complex interplay of factors such as production scheduling, raw material characteristics, process parameters, and equipment condition. This study proposes a novel approach to predict HEC (GJ/t) by utilizing actual production data from SRRF. A genetic algorithm (GA) optimized back-propagation neural network (BPNN) is developed and its performance is compared to that of a standard BP model. Experimental results reveal that the optimized GA-BP model, with a neural network structure of 17-10-1, achieves a prediction accuracy of 94.7% surpassing the 90.24% accuracy of the standard BP model. The proposed GA-BP model demonstrates superior predictive capabilities and robustness, offering valuable insights for optimizing process parameters and improving energy efficiency in SRRF operations.

Keywords Heat energy consumption per ton of steel billet, Prediction model, Genetic algorithm, Steel rolling reheating furnace

General introduction

Amid the intensifying global energy crisis and worsening environmental degradation, implementing energy-saving and emission-reduction strategies has become essential for achieving sustainable development goals¹⁻³. As a pillar of the manufacturing sector and national economies^{4,5}, the iron and steel industry represents one of the most energy-intensive sectors⁶, accounting for approximately 5% of global energy consumption^{7,8}. However, the industry grapples with significant challenges related to pollution and emissions⁹. Despite these challenges, substantial opportunities remain for energy conservation and emission reduction within the sector.

Research background

The Steel Rolling Reheating Furnace (SRRF), a critical component of the iron and steel rolling process^{10,11}, plays a vital role in achieving the required initial rolling temperature of billets¹². Consuming 15–20% of the total energy in iron and steel production and approximately 60–70% of the energy used in the rolling process^{13–15}, optimizing SRRF energy efficiency is essential for improving energy utilization and promoting sustainability in steel production.

Effective energy management is crucial in energy-intensive industries such as steel production^{16,17}. A key metric for SRRF optimization is the Heat Energy Consumption per ton of steel billet, abbreviated as HEC (measured in GJ/t). Hereafter, this metric will be referred to as HEC (GJ/t) for simplicity. This metric significantly impacts product quality, production costs, and energy management. However, identifying the factors contributing to HEC (GJ/t) fluctuations remains challenging due to the complex interactions among various operational parameters. Traditional methods fail to comprehensively and quantitatively assess energy utilization, highlighting the need for innovative approaches.

Research contributions

This study presents a hybrid GA-BP model for predicting the heat energy consumption of billets during the reheating process in steel rolling. Utilizing actual production data from a steel plant and integrating equipment and operational parameters, the proposed model enhances prediction accuracy and offers actionable insights for optimizing SRRF operations. Unlike conventional methods, the GA-BP model integrates energy management

School of Energy and Environment, Anhui University of Technology, Ma'anshan 243002, Anhui Province, People's Republic of China. [✉]email: 769305363@qq.com

with advanced machine learning techniques, providing a novel and systematic approach to energy efficiency management in the steel industry.

The key contributions of this research are given as follows:

- *Methodological innovation:* This study pioneers the integration of GA and BPNN for predicting HEC (GJ/t) in SRRF, marking the first application of this combined approach. Existing research in the steel industry lacks such a combined approach for accurately forecasting and managing the energy consumption of heating furnaces. Our innovative method integrates traditional energy management strategies with data-driven machine learning techniques, addressing this critical gap and offering a novel solution. It provides fresh perspectives and opens new possibilities for accurate energy consumption prediction and efficient management in SRRF, establishing itself as a distinct and valuable contribution to the field.
- *Model enhancement:* By using GA to optimize BPNN initialization, we effectively mitigate its sensitivity to initial weights and reduce the risk of being trapped in local optima. This optimization substantially improves the model's robustness and prediction accuracy, offering a more reliable and precise tool for estimating HEC (GJ/t) in SRRF.
- *Industry impact:* The proposed model offers robust, data-driven support for optimizing SRRF operations. By accurately predicting HEC, it empowers steel manufacturers to make informed decisions about parameter adjustments and production planning. This not only reduces production costs but also plays a vital role in advancing sustainable steel production practices, contributing to the industry's long-term environmental and economic sustainability.

The remainder of this paper is organized as follows: Section “[Literature review](#)” reviews and analyzes existing research on heating furnaces, highlighting the novelty and contributions of this study. Section “[Problem description](#)” outlines the research problem and provides details on the data sources and datasets used in this study. It also presents the modeling methods, describing the construction of the GA-BP model, parameter settings, and evaluation metrics. Section “[Results and performance analysis](#)” presents the results and analysis, covering model training, performance evaluation, error analysis, and regression analysis to validate the proposed model's effectiveness. Section “[Managerial insights and practical implications](#)” discusses the model's contributions, focusing on managerial insights and practical applications. Section “[Conclusions and perspectives](#)” summarizes the study and offers directions for future research.

Literature review

Related research on SRRF

The potential for energy savings and emission reductions in SRRF has been demonstrated through structural improvements^{18,19}, operational refinements^{20,21}, and enhanced management practices²². Among these, HEC (GJ/t) serves as a simple yet comprehensive metric for evaluating energy efficiency^{23,24}. Specifically, the allocation of HEC (GJ/t) for billets in SRRF is influenced by furnace gas fuel consumption and billet output. This metric plays a crucial role in analyzing energy consumption patterns and guiding optimization strategies.

The complexity of energy consumption in SRRF arises from the interplay of numerous factors and their intricate operational mechanisms. Currently, energy management in the industry often operates independently of advanced information technologies, resulting in inaccuracies in parameter analysis and inefficiencies in performance evaluations²⁵.

The highly non-linear and coupled relationships between HEC (GJ/t) and its influencing factors complicate conventional analysis methods^{26,27}. The relationship between these diverse factors and HEC (GJ/t) is highly intricate, exhibiting pronounced non-linearity and coupling. Conventional theories and mechanistic methods have struggled to effectively elucidate the coupling relationship and patterns of variation between HEC (GJ/t) and its influencing factors²⁸. Consequently, there is an increasing demand for advanced modeling techniques capable of capturing these relationships.

Related research on machine learning

In the field of applying machine learning to heating furnace research, numerous scholars have conducted extensive investigations^{29–31}. Among the various methods explored, the Back Propagation Neural Network (BPNN) has gained significant attention due to its exceptional ability to model nonlinear relationships^{32–34}.

For example, Wang and Hou³⁵ used actual production data from the SRRF process and applied the BPNN approach to model billet tapping temperatures, yielding promising results. However, the BPNN is subject to inherent limitations. It is highly sensitive to initial weights and thresholds, and it is prone to getting trapped in local optima.

To address the limitations of the BP neural network, some scholars have introduced optimization algorithms. Jiang and Li³⁶ applied the particle swarm optimization (PSO) algorithm to optimize the BPNN, allowing the PSO-BP neural network to outperform the traditional BPNN in terms of prediction accuracy and convergence speed. Similarly, Sun and Yu³⁷ optimized the BPNN using the Ant Colony Algorithm to develop a model for predicting billet tapping temperatures, successfully meeting actual production requirements.

In addition to optimizing the BPNN, some scholars have explored alternative approaches. Zhou and Zheng³⁸ combined the Improved Pelican Optimization Algorithm (IPOA) with Long Short-Term Memory (LSTM) to predict billet tapping temperatures. They further developed the model by incorporating Principal Component Analysis and other techniques, achieving excellent performance. Bao and Zhang³⁹ proposed a partition model based on multiple linear regression with variable parameter space-time (MLR-VPST) to predict the temperature distribution within the SRRF. Additionally, Kim and Moon⁴⁰ developed an improved modular neural network for monitoring the SRRF, capable of determining the optimal dimensions to describe its dynamic behavior.

Overall, a significant portion of these studies has focused on the temperature of the SRRF, particularly emphasizing billet tapping temperatures. This temperature is a critical indicator of the operation and quality control of the heating furnace process, reflecting heating efficiency and directly impacting the subsequent processing of the billet.

Research gap

A comparative overview of relevant research on SRRF is provided in Table 1. Although some scholars have employed optimization methods, these studies primarily focus on billet tapping temperature as the prediction index, with limited attention given to the overall energy consumption index of SRRF. Energy consumption in SRRF plays a crucial role in cost control and the sustainable development of steel production, and accurately predicting this index forms a critical foundation for production optimization.

In contrast, while some scholars have applied GA to optimize the BP neural network in certain contexts, a significant gap remains in existing research regarding the prediction of energy consumption in Steel Rolling Reheating Furnaces (SRRF) using data-driven methods. This study fills this gap by leveraging a GA-optimized BP neural network to predict the energy consumption of SRRF, presenting a novel approach within this specific domain.

The GA, when used to optimize the BP neural network, especially considering the complex scenarios of SRRF energy consumption prediction where multiple factors interact intricately to form highly nonlinear relationships, offers distinct advantages over other algorithms⁴¹, which are elaborated as follows:

- *Superior diversity maintenance*: Compared to the Particle Swarm Optimization algorithm, GA simulates natural selection and genetic mechanisms. This unique feature ensures better maintenance of population diversity during the search process, effectively mitigating the risk of premature convergence to local optima. Consequently, GA allows for a more thorough exploration of the solution space, increasing the likelihood of finding optimal or near-optimal solutions for complex problems such as SRRF energy consumption prediction.
- *Higher efficiency in large-scale problems*: Compared to the Ant Colony Optimization algorithm, GA demonstrates greater efficiency in handling large-scale problems associated with SRRF energy consumption prediction. Its ability to rapidly navigate complex solution landscapes makes it a more suitable choice for addressing the intricate nonlinear relationships inherent in this context. This capability enables faster and more accurate predictions, which are crucial for real-time decision-making in industrial settings.
- *Established theoretical foundation and rich experience*: Compared to the Improved Pelican Optimization Algorithm (IPOA), GA offers a more robust theoretical foundation and extensive application experience. Its well-defined selection, crossover, and mutation operations provide it with greater comprehensiveness and flexibility in exploring diverse solution spaces. These features make GA particularly well-suited for addressing the complex nonlinear dynamics of heating furnace energy consumption, allowing for more accurate and reliable predictions.

This research is highly significant as it successfully addresses the long-standing gap in data-driven prediction of SRRF energy consumption. By pioneering the application of the GA-BP algorithm, our research introduces a novel and practical solution for accurately predicting the HEC (GJ/t) of SRRF. This innovative approach not only offers a fresh perspective but also provides crucial data-driven support for optimizing SRRF operations, addressing aspects that have been underexplored in previous studies. Specifically, the key innovations and contributions of this research are outlined as follows:

- *Comprehensive factor consideration*: For the first time, the GA-BP algorithm is used to predict the HEC of SRRF, considering a comprehensive range of influencing factors in the SRRF production process. This holistic approach greatly improves the reliability of predictions by capturing the complex interactions between various operational parameters. By taking multiple factors into account simultaneously, the model offers a

Reference	Methodology	Specific method	Case study	Model basis
¹⁸	Simulation	CFD	Scale formation	Mechanism model
¹⁹	Design	Optimized Design	Design of burner	Mechanism model
²⁰	Simulation	CFD	Process simulation in furnace	Mechanism model
²¹	Theoretical analysis	Nonlinear model	Analysis of energy flow and efficiency of SRRF	Mechanism model
²²	Theoretical analysis	Weighted sum of gray gas model	Performance of SRRF	Mechanism model
³⁵	Machine learning	BPNN	Prediction of billet tapping temperature	Data model
³⁶	Machine learning	BPNN, PSO	Prediction of billet tapping temperature	Data model
³⁷	Machine learning	BPNN, CA	Prediction of billet tapping temperature	Data model
³⁸	Machine learning	IPOA, LSTM, PCA	Prediction of billet tapping temperature	Data model
³⁹	Machine learning	MLR-VPST	Temperature distribution within the SRRF	Data model
⁴⁰	Machine learning	Modular neural network	Describe the dynamic behavior of the SRRF	Data model
This research	Machine learning	BPNN, GA	Prediction of energy consumption of SRRF	Data model

Table 1. Related works. Significant values are in bold.

more accurate depiction of real-world scenarios, leading to more informed decision-making in production optimization.

- *Robust model optimization:* The GA optimizes the initial parameters of the BP neural network, improving its robustness and prediction accuracy. By avoiding local optima, the model provides more accurate and stable predictions of HEC, which is essential for practical applications in steel production. This optimization not only enhances the model's performance but also improves its generalization capability, making it suitable for a broader range of production conditions.
- *Practical operational support:* Based on actual production data, the model effectively captures the complex, nonlinear relationships among various factors. It provides actionable, data-driven support for parameter adjustment and production optimization, enabling steel plants to develop more effective operational strategies for sustainable production. This practical aspect addresses a significant gap in previous theoretical or partially operational studies, offering a tangible solution for improving energy efficiency and sustainability in steel manufacturing processes.

Problem description

This study aims to accurately predict the HEC (GJ/t) of SRRF using a data-driven approach, leveraging historical data from SRRF. Rather than relying solely on traditional laboratory experiments, this study provides a field-based alternative. It utilizes operational data directly collected from the SRRF production environment in domestic steel mills. This dataset captures real-time production information, reflecting the dynamic conditions of the reheating process. Unlike controlled laboratory settings, this “field experiment” approach ensures greater authenticity and robustness, better representing real-world operations.

The SRRF is structurally divided into distinct zones along its length: the preheating section, the first and second heating sections, and the soaking section.

Data resource

These zones correspond to distinct stages of billet heating, each with its own unique operating characteristics and energy consumption patterns. The factors influencing the HEC (GJ/t) are categorized into billet attribute parameters and operational parameters, comprising a total of 17 key factors (Fig. 1). These include billet size, heating mode, and equipment performance, all of which are widely recognized in the industry as critical determinants of furnace energy efficiency.

A data-driven approach was employed to predict billet energy consumption by considering the interplay of multiple variables. Including all 17 factors ensures that their complex interactions are captured, thereby enhancing the comprehensiveness and accuracy of the model. The dataset consists of 1200 data samples, divided into training, validation, and test subsets in proportions of 75%, 15%, and 10%, respectively, to ensure effective model performance evaluation.

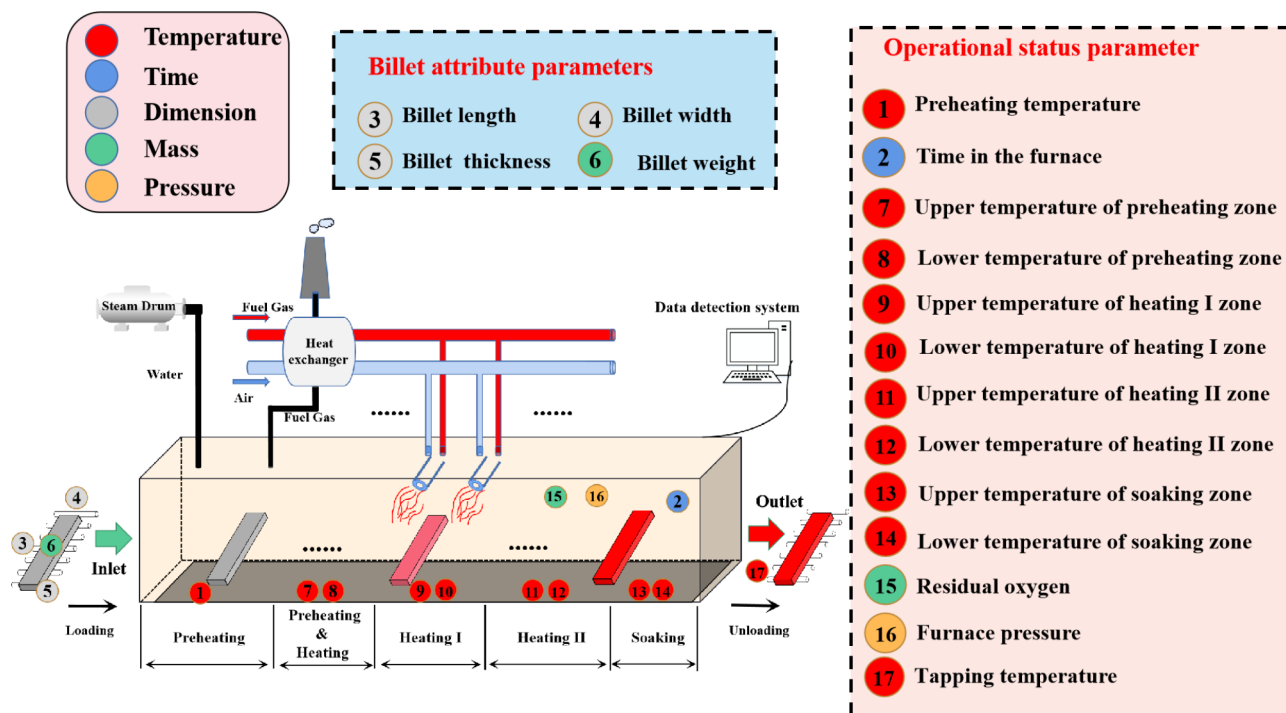


Fig. 1. Schematic illustration of the SRRF structure and factors affecting HEC (GJ/t).

Method**Indices**

t Set of influence factors; $t \in T = [1, 17]$,
 i Set of sample serial number; $i \in n = [1, 2, \dots, n]$,

Parameters

s Influence factor; (Influence factor t),
 u Number of input layer nodes,
 l Number of hidden layer nodes,
 m Number of output layer nodes,
 a Adjustment constant; ($1 \leq a \leq 10$),
 $f()$ Is the single-level Active function of the transfer function from the input layer to the hidden layer and from the hidden layer to the output layer of the BPNN,
 $F(X)$ Is the relationship between the input and the output,
 W Weight matrix of the input layer and the hidden layer,
 b_1 Threshold of the hidden layer,
 b_2 Threshold of the output layer,
 V Weight matrix of the hidden layer and the output layer,
 P Initial population size,
 e Maximum evolutionary epochs,
 cro Crossover probabilities,
 mu Mutation probabilities,
 $Goal$ Minimum training error target,
 $Epochs$ Maximum number of network training iterations,
 $Show$ Display frequency of training process,
 Lr Learning rate,
 Mc Momentum factor,
 Min_grad Minimum performance gradient,
 Max_fail Maximum number of consecutive training failures,

Variables

n Is the sample size of the data set;
 x_i Sample data(sample group i); (A set of data contains 17 influencing factors.)
 y_i Actual value of HEC (GJ/t)(Actual value of the i sample);
 \hat{y}_i Predicted value of HEC (GJ/t)(Predicted value of the i sample);
 z Original data,
 Z_{max} Maximum value of the sample,
 Z_{min} Minimum value of the sample,
 Z Normalized data,
 X Input vector; $X = [s_1, s_2, \dots, s_{17}]^T$,
 Y Output vector; $Y = [\hat{y}]$,
 MS Mean Square Error of HEC (GJ/t) between actual value and predicted values,
 $MAPE$ Mean Absolute Percentage Error of HEC (GJ/t) between actual value and predicted values,
 $RMSE$ Root Mean Square Error of HEC (GJ/t) between actual value and predicted values,
 R Correlation Coefficient.

BP neural network structure

Figure 2 illustrates the topological structure of a three-layer BPNN. The general signal forward propagation process is presented in Eq. (1). The training process of this model is divided into three stages:

1. *Input stage*: Data from 17 factors influencing HEC (GJ/t) in SRRF are fed into the network.
2. *Error evaluation*: The network output is compared with the actual HEC (GJ/t) data, and the prediction error is assessed using an objective function.
3. *Weight adjustment*: Weights and thresholds are updated through backpropagation to iteratively minimize the prediction error.

$$Y = F(X) = f[V \cdot f(W \cdot X + b_1) + b_2] \quad (1)$$

Genetic algorithm optimized BP neural network

The Genetic Algorithm (GA) is an adaptive heuristic search method based on Darwinian natural selection principles. It simulates biological processes such as replication, crossover, and mutation to efficiently and globally solve optimization problems^{42,43}. Starting from an initial population, the GA iteratively generates individuals with higher fitness through selection, crossover, and mutation operations, ultimately converging to an optimal solution (Fig. 3).

Proposed model

While the BP neural network is effective for prediction tasks, it is susceptible to local optima and slow convergence during gradient descent. To address these limitations, the GA optimizes the initial weights and thresholds of the

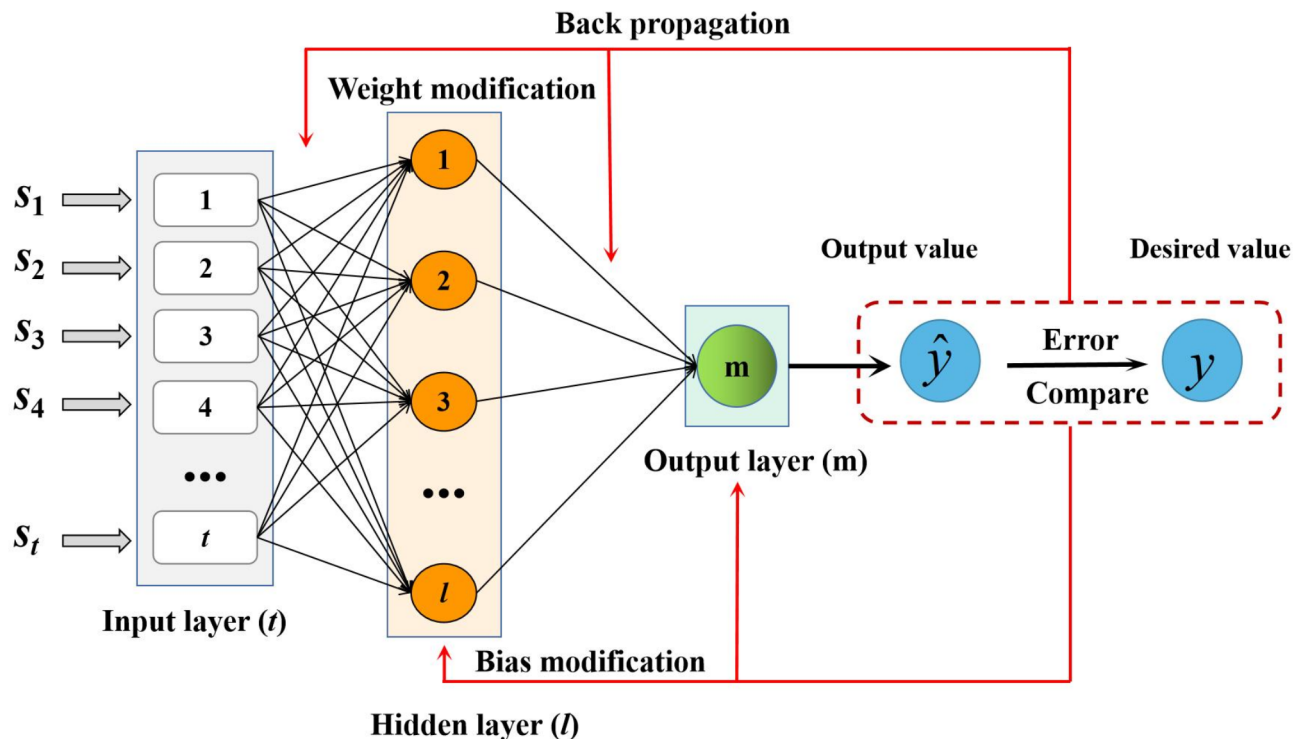


Fig. 2. Schematic diagram of the BP neural network topology.

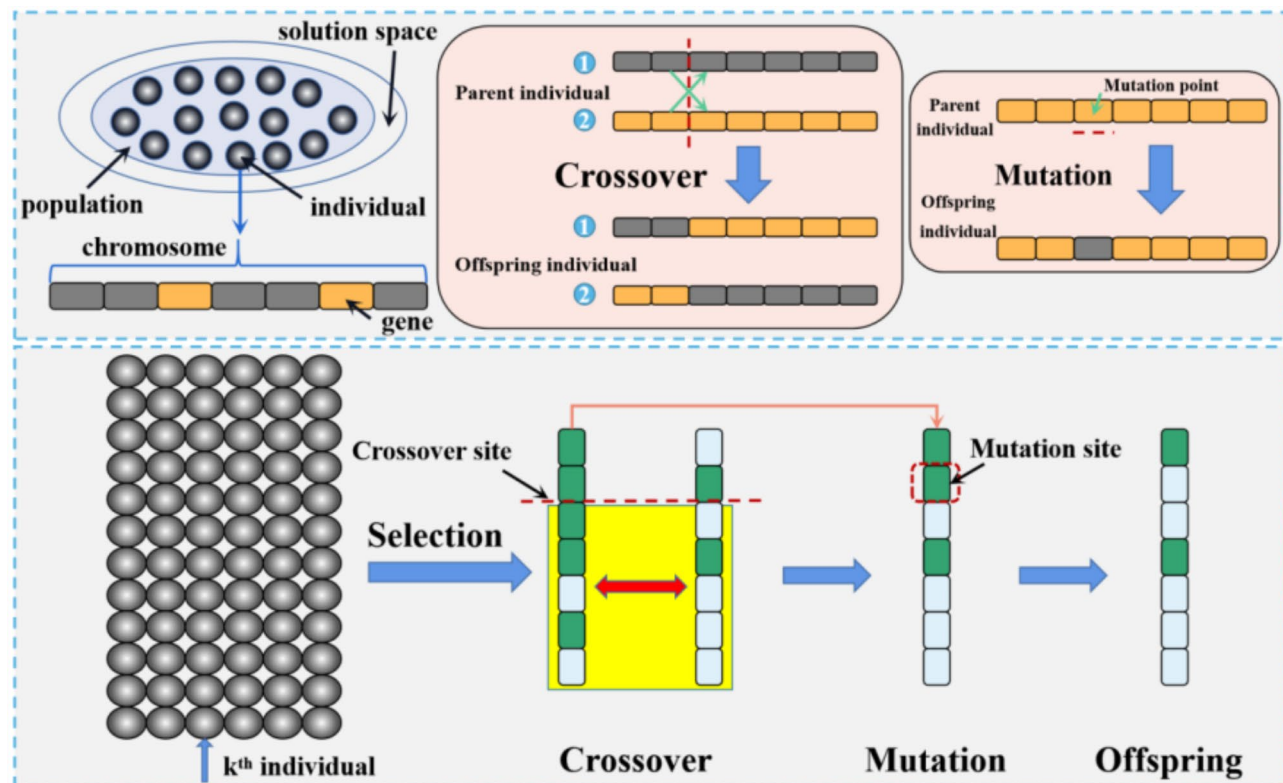


Fig. 3. Schematic diagram of selection, crossover, and mutation operations in the genetic algorithm.

BP network, enhancing stability and convergence speed. This hybrid GA-BP method is used to predict HEC (GJ/t) in SRRF. The overall training process is illustrated in Fig. 4.

The process of optimizing the BP neural network based on the genetic algorithm is as follows:

- (1) *Determining the neural network topology:* In the BP neural network model, the input layer consists of 17 factors influencing the HEC (GJ/t) for each dataset group, while the output layer represents the HEC (GJ/t). Therefore, the number of nodes in the input and output layers of the BP neural network structure is 17 and 1, respectively. The approximate range of nodes in the hidden layer is determined using empirical Formula 2. Ultimately, the number of hidden layer nodes is set to 10 through the trial-and-error method, guided by the RMSE index analysis. The process and results are illustrated in Fig. 5;

$$l < \sqrt{u + m} + a \quad (2)$$

- (2) *Data preprocessing:* To eliminate the impact of different data dimensions, the input data is normalized, as shown in Eq. (3);

$$Z = \frac{z - z_{\min}}{z_{\max} - z_{\min}} \quad (3)$$

- (3) The genetic algorithm procedures include determining the initial population size, setting evolutionary epochs, evaluating fitness, and performing selection, crossover, and mutation. Specific parameter settings are provided in Table 2. The fitness function value is calculated as the average Mean Squared Error (MSE) across both the training and test datasets. A smaller fitness function value indicates better training precision and higher prediction accuracy. The selection operation in the genetic algorithm uses the roulette wheel method, with crossover and mutation probabilities set to 0.8 and 0.2, respectively.
- (4) The BP neural network is constructed using the optimal initial weights and thresholds determined through iterative optimization. As shown in Fig. 5, the optimal number of nodes in the hidden layer of the BP neural network is 10, with 17 nodes in the input layer and 1 node in the output layer. Therefore, the structure of the BP model is 17-10-1. There are 180 weights ($17 \times 10 + 10 \times 1 = 180$) and 11 thresholds ($10 + 1 = 11$). Thus, the individual encoding length of the GA-BP neural network is 191 ($180 + 11 = 191$).
- (5) Import the training data to train the BP neural network model.
- (6) Input the data of the test set into the trained neural network for testing, and perform denormalization on the predicted data.

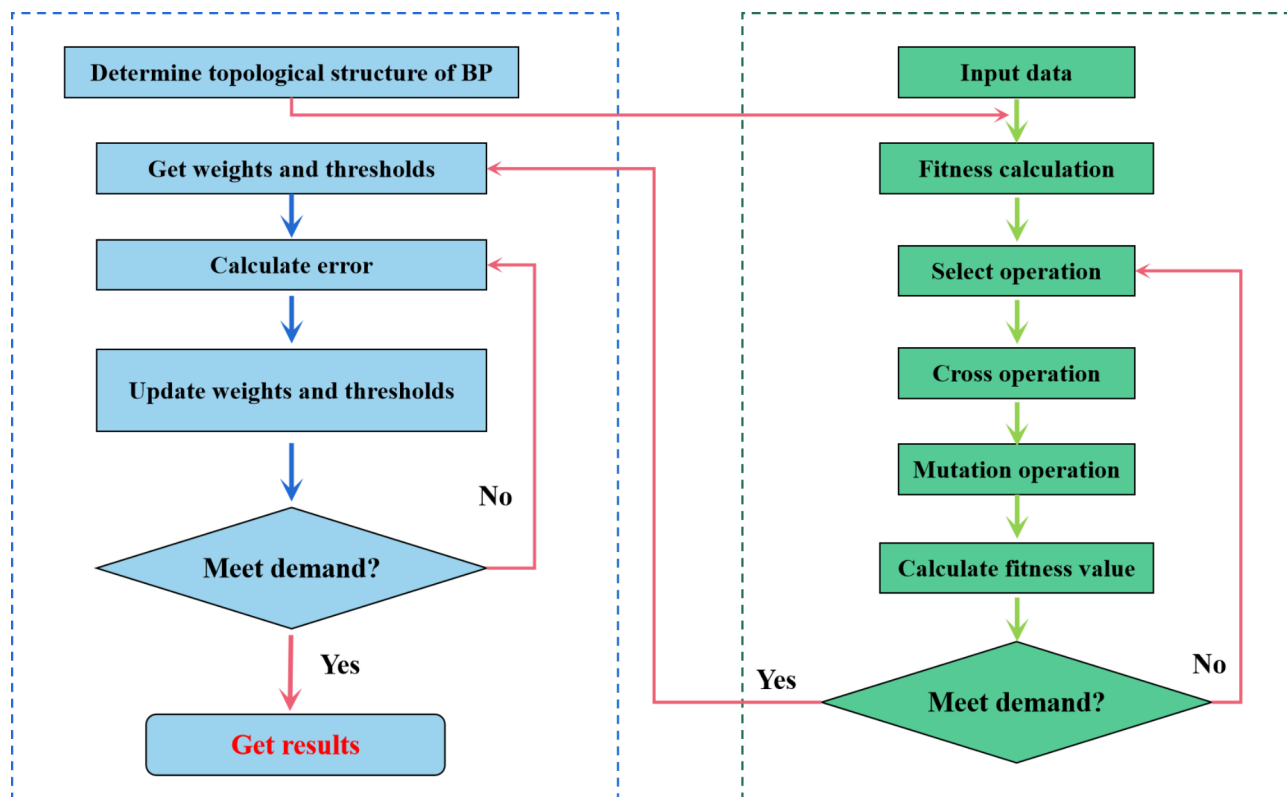


Fig. 4. Flowchart of the GA-BP neural network training process.

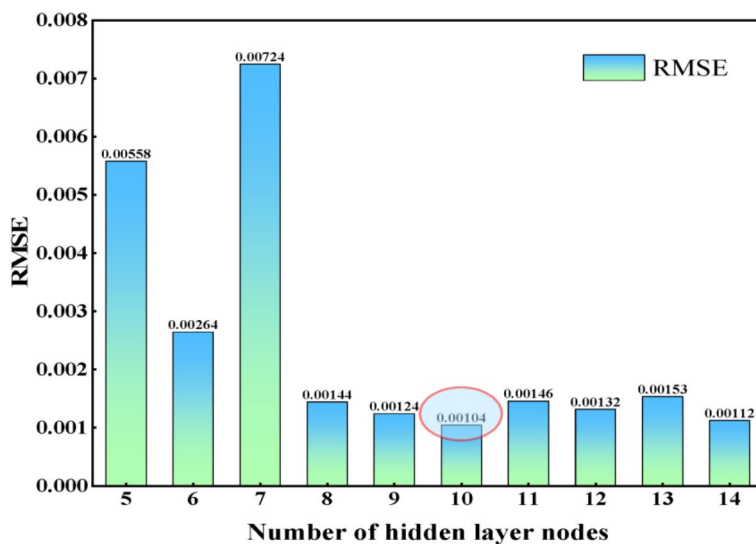


Fig. 5. RMSE of the model with different number of hidden layer nodes.

Parameter	Value
Initial population size (P)	30
Maximum evolutionary epochs (e)	60
Crossover probabilities (cro)	0.8
Mutation probabilities (mu)	0.2

Table 2. Parameter setting of genetic optimization algorithm.

Parameter	Value
Training goal minimum error (Goal)	0.00001
Maximum training times (Epochs)	1000
Learning rate (Lr)	0.01
Momentum factor (Mc)	0.1
Minimum performance gradient (Min_grad)	10^{-6}
Maximum number of failures (Max_fail)	6
Training iteration display frequency (Show)	25
Activation function ($f(\cdot)$)	Sigmoid

Table 3. Parameter setting for the BP and GA–BP model.

(7) Perform an error analysis by comparing the predicted values with the actual values obtained.

GA-BP model parameter setting and evaluation index selection

Training is performed using the Levenberg–Marquardt algorithm, with the parameter settings of the GA-BP model detailed in Table 3. Model validation is carried out using RMSE and MAPE, as defined in Eqs. (4 and 5), respectively.

$$\text{RMSE} = \sqrt{\frac{1}{n} \sum_{i=1}^n (y_i - \hat{y}_i)^2} \quad (4)$$

$$\text{MAPE} = \frac{100\%}{n} \sum_{i=1}^n \left| \frac{\hat{y}_i - y_i}{y_i} \right| \quad (5)$$

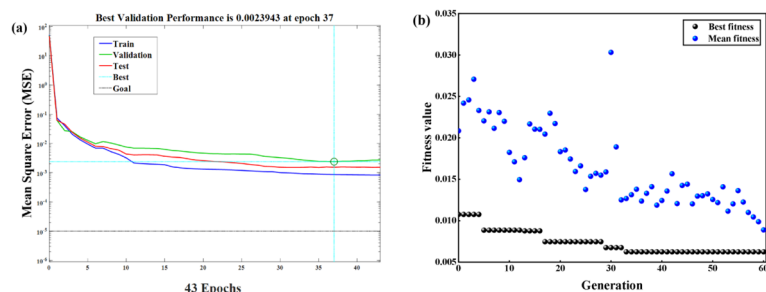


Fig. 6. Train the optimization process. (a) Mean square error of training set, verification set and test set. (b) Genetic algorithm optimization process diagram.

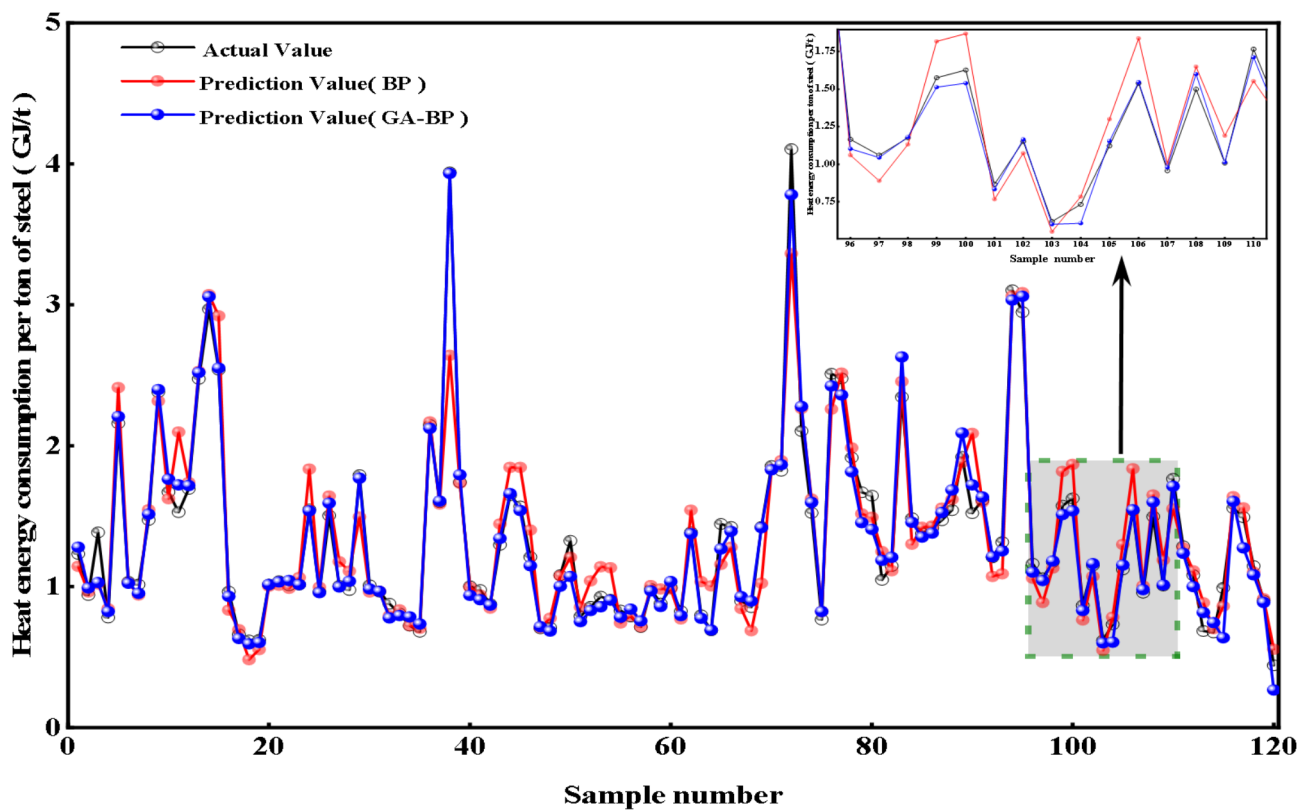


Fig. 7. Comparison of predicted and actual values between BP model and GA-BP model.

Results and performance analysis

Optimization process

The sample data is divided into training, validation, and test datasets. The training dataset is used to train the prediction model, while the validation and test datasets are used to evaluate and verify the accuracy of the GA-BP model. Figure 6a presents the MSE during the iterative optimization process for the training, validation, and test datasets. The error decreases with additional training iterations, reaching its minimum value of 0.0023943 for the validation dataset MSE at the 37th generation.

The optimization process of the genetic algorithm is illustrated in Fig. 6b. The process begins with an initial population size of 30 and a maximum of 60 evolutionary epochs, with a crossover probability of 0.8 and a mutation probability of 0.2. The population shows an average fitness of 0.0164, and the highest fitness is achieved in the 33rd generation, with an optimal value of 0.00624.

Results and analysis

Simulation results

The predictive performance of the developed model was evaluated using the test dataset. Figure 7 illustrates the actual value curve and the prediction curve for HEC (GJ/t) produced by both the BP model and the GA-BP model. Across 120 samples in the test set, the actual HEC (GJ/t) values exhibit fluctuations according to

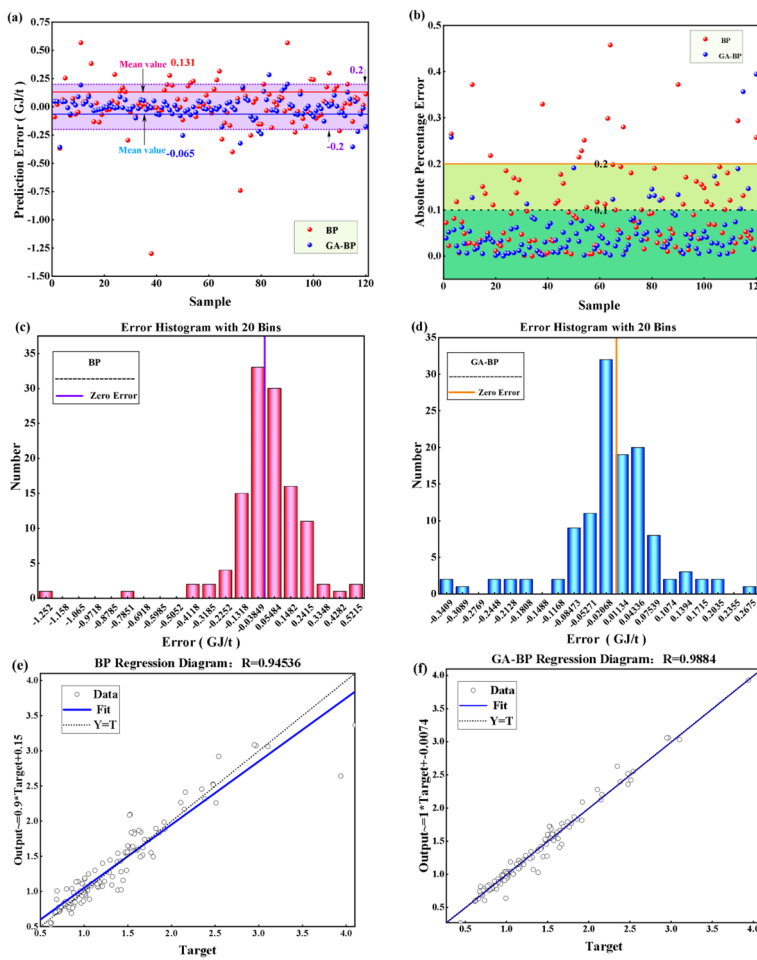


Fig. 8. Performance analysis. (a) Prediction Error. (b) Absolute Percentage. (c) BP error distribution. (d) GA-BP error distribution. (e) Correlation coefficient in BP model. (f) Correlation coefficient in GA-BP model.

the sample number. Both models effectively capture the underlying trends and patterns. However, a detailed comparison reveals that the GA-BP model, optimized through a genetic algorithm, demonstrates superior prediction accuracy and alignment with the actual values. In contrast, the conventional BP model, while capturing overall trends, lacks precision. The MAPE was used to quantify prediction accuracy. The original BP neural network achieved an accuracy of 90.24%, while the GA-BP model attained 94.75% accuracy on the test dataset. The GA-BP model's optimization minimizes prediction errors, enabling accurate predictions of HEC (GJ/t) values and meeting the desired accuracy objective.

To maintain data integrity and ensure realistic applicability in industrial scenarios, the collected data were normalized without removing outliers. This approach reduces the risk of overfitting and enhances the generalization performance of the trained model in real-world applications.

>Error analysis

The majority of prediction errors for the GA-BP model fall within the range of -0.2 to 0.2 GJ/t. Only a small fraction of prediction errors deviate beyond this range, compared to a notably higher frequency of such deviations in the BP model. The average prediction errors for the GA-BP and BP models are -0.065 and 0.131, respectively (Fig. 8a). As shown in Fig. 8b, the sample point distribution of the GA-BP model is predominantly concentrated within the dark green area, corresponding to an absolute percentage error of less than 0.1. In contrast, the BP model displays a more scattered sample point distribution, with several points located beyond the reference line. These findings highlight the GA-BP model's ability to reduce both error magnitude and variability, significantly enhancing prediction accuracy⁴⁴.

Figure 8c,d illustrate the error distribution histograms for the two models. The BP model exhibits an error range from -1.252 to 0.522 GJ/t (Fig. 8c), as indicated by the purple vertical reference line at zero error. In contrast, the GA-BP model achieves a narrower error range of -0.3409 to 0.2675 GJ/t (Fig. 8d), with the orange vertical line representing zero error. The narrower range and more uniform distribution demonstrate the GA-BP model's effectiveness in reducing prediction error.

Regression analysis

The correlation coefficient serves as a key metric for evaluating model performance, quantifying the linear relationship between the model's predicted results and the observed values⁴⁵. Figure 8e,f highlight a clear contrast in data fitting between the BP neural network and the GA-BP neural network. Notably, the GA-BP model demonstrates superior fitting performance, with a correlation coefficient (R) of 0.9884 (Fig. 8e), outperforming the BP model, which has a coefficient of 0.94536 (Fig. 8f). This improvement highlights the GA-BP model's superior ability to capture linear relationships in the data. The enhanced performance of the GA-BP model is attributed to the optimization capabilities of the genetic algorithm, which efficiently explores the parameter space and identifies optimal configurations. In contrast, the traditional BP model tends to get trapped in local optima, restricting its predictive performance.

Managerial insights and practical implications

In steel production, the GA-BP model accurately predicts the HEC (GJ/t) of SRRFs, aiding in strategic production scheduling. Managers can optimize batches using these predictions, reducing energy waste, minimizing idle time, and increasing throughput.

As energy costs constitute a significant portion of steel production expenses, the GA-BP model factors in risk elements, enabling precise energy budgeting. By optimizing the fuel mix, adjusting parameters, and scheduling off-peak maintenance, costs can be reduced, leading to enhanced enterprise efficiency.

As a reliable SRRF performance evaluation tool, the GA-BP model compares actual and predicted consumption, helping to identify issues such as equipment failures and inefficiencies. This allows for the establishment of realistic targets, improving quality control and maintenance.

Amid environmental and competitive pressures, the model aids enterprises in navigating energy price fluctuations and regulations. Its predictions inform investments in energy-saving technologies and upgrades, enhancing both reputation and competitiveness. The model's application contributes to technological advancements and sustainability within the steel industry, helping to reduce emissions. Furthermore, its approach provides valuable insights for energy management in other industries, such as metallurgy and chemical engineering, fostering energy optimization across sectors.

In conclusion, managers and policymakers should adopt the GA-BP model and integrate it into decision-making to make informed, efficient, and sustainable choices that benefit enterprises, the industry, and society.

Conclusions and perspectives

Conclusions

Considering the nonlinear, strongly coupled, and highly complex nature of calculating the Heat Energy Consumption per ton (HEC, GJ/t) in a Steel Rolling Reheating Furnace (SRRF), a prediction model for HEC (GJ/t) has been established. This model integrates a Back Propagation (BP) neural network optimized using a genetic algorithm (GA). By employing 17 process parameters as input features and setting the predicted HEC (GJ/t) as the output, the following model details were determined:

The key findings of this study are summarized as follows:

- *Determination of the optimal model structure:* Through a series of trial-and-error experiments, the optimal structure of the BP model, denoted as (17-10-1), was determined. This structure consists of 17 input features derived from process parameters, 10 neurons in the hidden layer, and 1 output representing the predicted HEC (GJ/t). This structure forms a solid foundation for the model's subsequent performance.
- *Exceptional model performance:* The GA-BP model significantly outperforms the conventional BP model in terms of prediction accuracy. The Mean Absolute Percentage Error (MAPE) of the BP model is 0.0976, while the GA-BP model achieves a MAPE of 0.0525, reflecting a 46.2% reduction in error. Furthermore, compared to the BP model, which has a regression coefficient (R) of 0.9454, the GA-BP model exhibits a narrower error range and a higher regression coefficient (R = 0.9884). Overall, the GA-BP model achieves a prediction accuracy of 94.7% for HEC (GJ/t) values, fully meeting the expected accuracy criteria.
- *Substantial application value:* This research provides valuable insights into process control and parameter optimization within SRRF operations. The accurate prediction of HEC (GJ/t) by the GA-BP model facilitates strategic production scheduling, enabling more efficient energy utilization and minimizing unnecessary energy waste. Additionally, by providing a better understanding of energy consumption patterns, the model enhances the operational reliability of SRRFs, supporting more informed decision-making in areas such as equipment maintenance and production planning. Consequently, it contributes to improved energy efficiency, leading to positive economic and environmental benefits for the steel production industry.

Perspectives

Expanding the research scope

Future research will focus on combining data-driven models with physics-based models to develop a hybrid forecasting framework. This dual-driven approach is expected to enhance the interpretability and stability of predictions, compensating for the limitations of purely data-driven methods. By integrating physical models or domain expertise, the explanatory power and generalizability of the predictive framework can be further improved.

Improving model performance

Future investigations will focus on optimizing feature selection to minimize redundancy and enhance predictive accuracy, particularly in high-dimensional data environments. Techniques such as dimensionality reduction and feature extraction will be employed to retain critical information. Additionally, more advanced machine

learning algorithms, such as deep learning and reinforcement learning, will be explored to enhance the model's adaptability and predictive performance.

Expanding practical applications

Efforts will be directed toward applying the developed model to broader industrial scenarios, including complex technological processes and dynamic environments. Systematic testing and experimental validation under various conditions will be conducted to evaluate the robustness and generalizability of the model. Collaborations with industry partners will focus on translating research findings into practical applications, promoting energy conservation, and improving efficiency in industrial processes.

Data availability

The datasets used and/or analysed during the current study available from the corresponding author on reasonable request.

Received: 21 May 2024; Accepted: 19 March 2025

Published online: 01 April 2025

References

- Wang, R. Q., Jiang, L., Wang, Y. D. & Roskilly, A. P. Energy saving technologies and mass-thermal network optimization for decarbonized iron and steel industry: A review. *J. Clean. Product.* **274**, 122997. <https://doi.org/10.1016/j.jclepro.2020.122997> (2020).
- Xiang, Q. et al. Impacts of energy-saving and emission-reduction on sustainability of cement production. *Renew. Sustain. Energy Rev.* **191**, 114089. <https://doi.org/10.1016/j.rser.2023.114089> (2024).
- Chang, Y., Wan, F., Li, J., Liu, N. & Yao, X. The impact of cautious coal power phase-out on decarbonization of China's iron and steel industry. *J. Clean. Product.* **397**, 136447. <https://doi.org/10.1016/j.jclepro.2023.1364476> (2023).
- Liu, Y. et al. Environmental and economic sustainability of key sectors in China's steel industry chain: An application of the Emergy Accounting approach. *Ecol. Indicat.* **129**, 108011. <https://doi.org/10.1016/j.ecolind.2021.108011> (2021).
- Yang, X. et al. Multinational dynamic steel cycle analysis reveals sequential decoupling between material use and economic growth. *Ecol. Econom.* **217**, 108092. <https://doi.org/10.1016/j.ecolecon.2023.108092> (2024).
- Fukuyama, H., Liu, H.-H., Song, Y.-Y. & Yang, G.-L. Measuring the capacity utilization of the 48 largest iron and steel enterprises in China. *Eur. J. Oper. Res.* **288**, 648–665. <https://doi.org/10.1016/j.ejor.2020.06.012> (2021).
- Chen, L., Yang, B., Shen, X., Xie, Z. & Sun, F. Thermodynamic optimization opportunities for the recovery and utilization of residual energy and heat in China's iron and steel industry: A case study. *Appl. Therm. Eng.* **86**, 151–160. <https://doi.org/10.1016/j.applthermaleng.2015.04.026> (2015).
- Chen, D., Lu, B., Dai, F., Chen, G. & Yu, W. Variations on billet gas consumption intensity of reheating furnace in different production states. *Appl. Therm. Eng.* **129**, 1058–1067. <https://doi.org/10.1016/j.applthermaleng.2017.10.096> (2018).
- Tan, Q., Liu, F. & Li, J. An integrated analysis on the synergistic reduction of carbon and pollution emissions from China's iron and steel industry. *Engineering* <https://doi.org/10.1016/j.eng.2023.09.018> (2023).
- Chakravarty, K. & Kumar, S. Increase in energy efficiency of a steel billet reheating furnace by heat balance study and process improvement. *Energy Rep.* **6**, 343–349. <https://doi.org/10.1016/j.egyr.2020.01.014> (2020).
- Zhao, J. et al. Industrial reheating furnaces: A review of energy efficiency assessments, waste heat recovery potentials, heating process characteristics and perspectives for steel industry. *Process Saf. Environ. Prot.* **147**, 1209–1228. <https://doi.org/10.1016/j.psep.2021.01.045> (2021).
- Ji, W., Li, G., Wei, L. & Yi, Z. Modeling and determination of total heat exchange factor of regenerative reheating furnace based on instrumented slab trials. *Case Stud. Thermal Eng.* **24**, 100838. <https://doi.org/10.1016/j.csite.2021.100838> (2021).
- Chen, D. et al. Fluctuation characteristic of billet region gas consumption in reheating furnace based on energy apportionment model. *Appl. Therm. Eng.* **136**, 152–160. <https://doi.org/10.1016/j.applthermaleng.2018.03.007> (2018).
- García, A. M., Colorado, A. F., Obando, J. E., Arrieta, C. E. & Amell, A. A. Effect of the burner position on an austenitizing process in a walking-beam type reheating furnace. *Appl. Therm. Eng.* **153**, 633–645. <https://doi.org/10.1016/j.applthermaleng.2019.02.116> (2019).
- Khalid, Y. et al. Oxygen enrichment combustion to reduce fossil energy consumption and emissions in hot rolling steel production. *J. Clean. Product.* **320**, 128714. <https://doi.org/10.1016/j.jclepro.2021.128714> (2021).
- Guang, F., Wen, L. & Sharp, B. Energy efficiency improvements and industry transition: An analysis of China's electricity consumption. *Energy* **244**, 122625. <https://doi.org/10.1016/j.energy.2021.122625> (2022).
- Aramendia, E., Brockway, P. E., Taylor, P. G. & Norman, J. Global energy consumption of the mineral mining industry: Exploring the historical perspective and future pathways to 2060. *Global Environ. Change* **83**, 102745. <https://doi.org/10.1016/j.gloenvcha.2023.102745> (2023).
- Landfahrer, M. et al. Numerical and experimental investigation of scale formation on steel tubes in a real-size reheating furnace. *Int. J. Heat Mass Transf.* **129**, 460–467. <https://doi.org/10.1016/j.ijheatmasstransfer.2018.09.110> (2019).
- Shanqing, X. & Daohong, W. Design features of air and gas double preheating regenerative burner reheating furnace. *Energy Procedia* **66**, 189–192. <https://doi.org/10.1016/j.egypro.2015.02.015> (2015).
- Mayr, B., Prieler, R., Demuth, M., Moderer, L. & Hohenauer, C. CFD analysis of a pusher type reheating furnace and the billet heating characteristic. *Appl. Therm. Eng.* **115**, 986–994. <https://doi.org/10.1016/j.applthermaleng.2017.01.028> (2017).
- Steinboeck, A., Wild, D. & Kugi, A. Energy-efficient control of continuous reheating furnaces. *IFAC Proc. Vol.* **46**, 359–364. <https://doi.org/10.3182/20130825-4-us-2038.00007> (2013).
- Han, S. H. & Chang, D. Radiative slab heating analysis for various fuel gas compositions in an axial-fired reheating furnace. *Int. J. Heat Mass Transf.* **55**, 4029–4036. <https://doi.org/10.1016/j.ijheatmasstransfer.2012.03.041> (2012).
- Zhang, Y. et al. Exergy and energy analysis of pyrolysis of plastic wastes in rotary kiln with heat carrier. *Process Saf. Environ. Prot.* **142**, 203–211. <https://doi.org/10.1016/j.psep.2020.06.021> (2020).
- Bao, X.-J. et al. Mechanism and application of an online intelligent evaluation model for energy consumption of a reheating furnace. *J. Iron. Steel Res. Int.* **30**, 102–111. <https://doi.org/10.1007/s42243-022-00801-8> (2022).
- Lu, B., Chen, D., Chen, G. & Yu, W. An energy apportionment model for a reheating furnace in a hot rolling mill—A case study. *Appl. Therm. Eng.* **112**, 174–183. <https://doi.org/10.1016/j.applthermaleng.2016.10.080> (2017).
- Gao, Q., Pang, Y., Sun, Q., Liu, D. & Zhang, Z. Modeling approach and numerical analysis of a roller-hearth reheating furnace with radiant tubes and heating process optimization. *Case Stud. Ther. Eng.* **28**, 101618. <https://doi.org/10.1016/j.csite.2021.101618> (2021).

27. Bao, Q., Zhang, S., Guo, J., Li, Z. & Zhang, Z. Multivariate linear-regression variable parameter spatio-temporal zoning model for temperature prediction in steel rolling reheating furnace. *J. Process Control* **123**, 108–122. <https://doi.org/10.1016/j.jprocont.2023.01.013> (2023).
28. Lu, B., Zhao, Y., Chen, D., Li, J. & Tang, K. A novelty data mining approach for multi-influence factors on billet gas consumption in reheating furnace. *Case Stud. Ther. Eng.* **26**, 101080. <https://doi.org/10.1016/j.csite.2021.101080> (2021).
29. Lotfi, R., Kheiri, K., Sadeghi, A. & Babaee Tirkolaee, E. An extended robust mathematical model to project the course of COVID-19 epidemic in Iran. *Ann. Operat. Res.* **339**, 1499–1523. <https://doi.org/10.1007/s10479-021-04490-6> (2022).
30. Lotfi, R. et al. A robust resilience machine learning with risk approach: A case study of gas consumption. *Ann. Oper. Res.* <https://doi.org/10.1007/s10479-024-05986-7> (2024).
31. Lotfi, R. et al. A robust and resilience machine learning for forecasting agri-food production. *Sci. Rep.* **12**, 21787. <https://doi.org/10.1038/s41598-022-26449-8> (2022).
32. Tian, W. & Cao, Y. Evaluation model and algorithm optimization of intelligent manufacturing system on the basis of BP neural network. *Intell. Syst. Appl.* **20**, 200293. <https://doi.org/10.1016/j.isma.2023.200293> (2023).
33. Chen, J. et al. Predict the effect of meteorological factors on haze using BP neural network. *Urban Clim.* **51**, 101630. <https://doi.org/10.1016/j.uclim.2023.101630> (2023).
34. Dodo, U. A. et al. Comparative study of different training algorithms in backpropagation neural networks for generalized biomass higher heating value prediction. *Green Energy Resour.* **2**, 10060. <https://doi.org/10.1016/j.gerr.2024.100060> (2024).
35. Wang, W., Hou, S., Wang, X. & Li, X. On neural network prediction model of billet temperature for 1700 reheating furnace in Tangsteel Company. *J. Univ. Sci. Technol. Liaoning* **46**, 189–193 (2017) (in Chinese).
36. Jiang, W., Li, H. & Liu, S. Prediction model of billet temperature in heating furnace based on PSO-BP neural network. *Energy Conserv.* **43**, 92–94 (2024) (in Chinese).
37. Sun, J. & Yu, M. Temperature neural network prediction model of billet in rolling heating furnace. *Foreign Electron. Measurement Technol.* **40**, 24–28. (in Chinese)
38. Zhou, J., Zheng, R. & Hou, H. Improved pelican algorithm for optimizing LSTM based temperature prediction of reheating furnace billets. *Foreign Electron. Measurement Technol.* **42**, 174–179 (2023) (in Chinese).
39. Bao, Q., Zhang, S., Guo, J., Li, Z. & Zhang, Z. Multivariate linear-regression variable parameter spatio-temporal zoning model for temperature prediction in steel rolling reheating furnace. *J. Process Control* **123**, 108–122. <https://doi.org/10.1016/j.jprocont.2023.01.013> (2023).
40. Kim, Y., Cheol Moon, K., Sam Kang, B., Han, C. & Soo Chang, K. Application of neural network to supervisory control of reheating furnace in steel industry. *IFAC Proc. Vol.* **30**, 33–38. [https://doi.org/10.1016/s1474-6670\(17\)44365-5](https://doi.org/10.1016/s1474-6670(17)44365-5) (1997).
41. Hu, Y., Tan, C., Broughton, J., Roach, P. A. & Varga, L. Model-based multi-objective optimization of reheating furnace operations using genetic algorithm. *Energy Procedia* **142**, 2143–2151 (2017).
42. Lee, C.-Y., Ho, C.-Y., Hung, Y.-H. & Deng, Y.-W. Multi-objective genetic algorithm embedded with reinforcement learning for petrochemical melt-flow-index production scheduling. *Appl. Soft Comput.* **159**, 111630. <https://doi.org/10.1016/j.asoc.2024.111630> (2024).
43. Zhu, J., Wang, G., Li, Y., Duo, Z. & Sun, C. Optimization of hydrogen liquefaction process based on parallel genetic algorithm. *Int. J. Hydrogen Energy* **47**, 27038–27048. <https://doi.org/10.1016/j.ijhydene.2022.06.062> (2022).
44. Kamel, B., Hamza, A. & Yahia, N. Modeling surface quality, cost and energy consumption during milling of alloy 2017A: A comparative study integrating GA-ANN and RSM models. *Int. J. Model. Simulat.*, 1–19, <https://doi.org/10.1080/02886203.2024.2320613> (2024).
45. Hamza, A., Dridi, I., Bousmina, K. & Ben Yahia, N. Active suspension for all-terrain vehicle with intelligent control using artificial neural networks. *J. Mech. Eng. Sci.*, 9883–9897, <https://doi.org/10.15282/jmes.18.1.2024.7.0782> (2024).

Acknowledgements

This work was supported by the National Key Research and Development Plan project (approval number: 2020YFB1711101) and the Anhui Province University Natural Science Research Project (Approval number: KJ2021A0411).

Author contributions

Yi Duan, Guang Chen, and Xiangjun Bao designed the study. Yi Duan and Guang Chen participated in the experiment. Yi Duan drafted the original draft, and Guang Chen and Xiangjun Bao provided guidance. Jing Xu, Lu Zhang and Xiaojing Yang provided constructive suggestions. All authors reviewed the manuscript.

Declarations

Competing interests

The authors declare no competing interests.

Additional information

Correspondence and requests for materials should be addressed to X.B.

Reprints and permissions information is available at www.nature.com/reprints.

Publisher's note Springer Nature remains neutral with regard to jurisdictional claims in published maps and institutional affiliations.

Open Access This article is licensed under a Creative Commons Attribution-NonCommercial-NoDerivatives 4.0 International License, which permits any non-commercial use, sharing, distribution and reproduction in any medium or format, as long as you give appropriate credit to the original author(s) and the source, provide a link to the Creative Commons licence, and indicate if you modified the licensed material. You do not have permission under this licence to share adapted material derived from this article or parts of it. The images or other third party material in this article are included in the article's Creative Commons licence, unless indicated otherwise in a credit line to the material. If material is not included in the article's Creative Commons licence and your intended use is not permitted by statutory regulation or exceeds the permitted use, you will need to obtain permission directly from the copyright holder. To view a copy of this licence, visit <http://creativecommons.org/licenses/by-nc-nd/4.0/>.

© The Author(s) 2025